

Chines-Dry Planing of Slender Hulls: A General Theory Applied to Prismatic Surfaces

John P. Breslin

Consultant and professor emeritus, Calle Dinamarca 7, San Miguel de Salinas, 03193 Alicante, Spain (formerly director, Davidson Laboratory and head of Ocean Engineering, Stevens Institute of Technology).

The ultimate goals of this two-part study are the advantages and deficiencies of application of camber to dry-chine, stepped-planing forms. The present paper is limited to the correlation of a relatively new theory with existing data to qualify it for use in a later paper which will predict the hydrodynamic characteristics of practical forms without and with cambers. Following a brief account of the pertinent literature, a mathematical model is developed via slender-body theory. It is a generalization of M. P. Tulin's (1957) seminal analysis of *flat*, cambered, delta-wing waterplanes to include deadrise, together with a departure from the oversimplified Wagnerian (1932) theory first introduced by Vorus (1996). It is an independent, less complicated development which confirms Vorus's result for his special case of straight-sided wedges. Detailed comparisons of all the hydrodynamic coefficients with data from model tests of prismatic hulls show that this theory is superior to that of Wagner. A very simple formula for maximum pressures is shown. Comparisons with the extensive theories of Zhao and Faltinsen are discussed. The theory is justified for extension to more pragmatic forms within the scope of the theory.

Introduction

THE ultimate principal objectives of this study are effects of camber on all hydrodynamic characteristics of slender, stepped-planing hulls of various shapes operating in the so-called chines-dry mode. Chine is defined by the knuckle formed by the intersection of the rise of the bottom and the more-or-less vertical side of a hull. Although extensive experimental and theoretical efforts have been devoted to the combined influences of trim and deadrise angles on lift, drag, pressure distribution, and center of lift of prismatic forms, relatively little has been done to explore benefits and deficiencies of longitudinal camber. Characterizations of the fluid dynamical aspects of prismatic surfaces, principally by model experiments, have provided the essential basis for pragmatic design of planing craft over many decades. Existing craft generally have lift-to-drag ratios around 8 or less, whereas experiments with cambered models of zero deadrise have shown values around 15. It would appear to be of use to explore the

possibility of drag reduction by application of relatively simple theory.

Planing may be defined to occur when the Froude numbers based on principal dimensions are sufficiently high that the weight of the craft is supported almost totally by the dynamic component of the pressure distribution, i.e., the static pressure is negligible. Another definition, adopted by Savitsky (1964), is related to the ventilation of the stern and the lift-drag ratio becomes independent of his speed coefficient. This definition requires the inclusion of gravity in the calculation of lift. Herein, the first definition is adopted as the inclusion of gravity at this stage needlessly complicates any mathematical model. Moreover, the speeds of major interest for planing in calm water ensure satisfaction of this criterion.

To a theorist, flow about a planing boat presents a nonlinear, free-boundary problem in a viscous fluid. Nonlinearity arises from the local distortion of the water surface which very importantly increases lift and wetted surface for the restrained hull. Viscosity must be allowed as experiments show that it is the cause of about 40% of the drag at optimum trim of prismatic forms! Nowadays it is the fashion to attack such formidable problems by application of boundary-element procedures involving huge matrices

Manuscript received at SNAME headquarters February 15, 2000; revised manuscript received July 25, 2000.

to invert two-dimensional integral equations with highly singular kernels, and to treat the viscous flows via Navier-Stokes equations with turbulence “models.” To be sure such methods must be used whenever assumptions for simpler mathematical modeling do not accommodate reality. Fortunately, because of practical considerations many planing hulls must be slender and operate at small trim angles from 3 to 6 deg and have deadrise angles decreasing from some 35 to 5 deg from bow to stern. These combinations generally result in waterplanes of aspect ratios of one or less, thereby opening the problem to application of slender-body and thin-section theory.

Following a brief review of the pertinent literature (as known by the author), construction of a model of the flow induced by a fairly general class of delta-wing like waterplanes in chines-dry mode is developed in detail. This model applies to the admittedly limited, but yet important, chines-dry operation because of the limitations of slender-body theory. This hull form is applicable to seaplanes and is not that which is widely employed in power boats that have waterplanes of delta-wing shape forward followed by a rectangular after-part. Herein the hull class is specialized to the very important family of prismatic forms for which data have been obtained from a systematic series of model tests. Successful correlations with these data are essential to justify the applicability of the theory to more general forms within its scope.

The theory developed herein is a generalization of Tulin’s (1957) work, described below, to model flow about slender hulls of triangular cross sections and varying deadrise angles. It is less general but simpler than Vorus’s (1996) model and is distinguished by initial emphasis on correlations with data and ultimate focus on effects of camber. This theory subsumes the old “expanding-plate” concept of Wagner (1932) without resorting to the descending wedge analogy and invoking change of added mass. The present paper terminates with a firm conclusion that because this theory agrees exceptionally well with data, it is a definite improvement over prior theory. It is justified for use in predicting the characteristics of more pragmatic forms with and

without camber, which is the subject of the second part of this study to appear in a separate paper.

Background and pertinent literature

There is a very large amount of literature on planing from experimental studies with models and theory extending over the past 90 years. Cited here are only those technical papers and reports which apply to the procedures used herein and the few studies which have been conducted on effects of camber.

As stated above, the present theory is a generalization of the seminal work by Tulin (1957). He demonstrated that the main features of the inviscid flow about slender, *flat* surfaces at high speed is well approximated by application of slender-body theory with an ingenious modification to give *finite* velocities along the waterlines. Moreover, he showed that camber reduces spray drag by reiterating the incisive, (but long-ignored!) observation of Wagner (1932) that the nonviscous drag of flat, slender planing forms is composed of induced drag and spray drag which are of equal magnitude in the absence of camber. Tulin gave results which showed that spray drag is a joint functional of the shapes of the waterplane and longitudinal camber, curvature and slope distribution. His parametric evaluations indicated that blunt forebodies with greater camber curvature aft would provide the least nonviscous drag. Tulin’s omission of frictional resistance did not give a realistic picture of the relative influence of lateral and vertical shapes on total drag. Nor did he compare with model data. A full, convex waterplane forward is unacceptable for operation in waves and would have considerably greater wetted surface and hence higher frictional drag than his concave waterplanes for the same lift.

Nevertheless, his work, though ignored by empiricists and theorists alike, inspired Vorus (1996) to develop a theory for vertical impact of symmetrical, two-dimensional wedges of curved and straight sides and to extend his procedure to inclined impact with others in Vorus et al (1998). His main departure from prior theory

Nomenclature

a = half-breadth of vorticity	g = acceleration due to gravity	β = constant deadrise angle; see Fig. 1
A_b = half-breadth attenuation with deadrise	F = Froude number	$\beta(x)$ = variable deadrise angle
A_R = aspect ratio = $\frac{(2b(l))^2}{\text{waterplane area}}$	J = Vorus’s wetting factor	β_c = effective β in presence of tapered camber; see equation (1)
$B(x, y)$ = Beta function	k = slope factor of tapered camber function	γ = local vorticity strength
$b_0(x)$ = static half-breadth of waterline	l = projected waterline length of keel	ϵ = dimensionless incremental extent of vorticity, $(a(x) - b(x))/b(x)$
$b(x)$ = dynamic half-breadth of waterplane at planing	L = lift	η = elevation of water surface
$c(x)$ = longitudinal distribution of camber	m = see sequel to equation (13)	λ = Savitsky’s mean wetted length in beams; $(2l_c + l)/4b(l)$
$C_{L_{lin}}$ = lift coefficient from linear part of pressure based upon l^2	$s = \left(\frac{v}{b(x)}\right)^2$	$\mu = \left(\frac{1}{2} - \frac{\beta}{\pi}\right)$; β radians
C_L = total- or net-lift coefficient	u = longitudinal component of induced velocity	$\nu = \left(\frac{1}{2} + \frac{\beta}{\pi}\right)$; also kinematic viscosity of water
$C_{L_{2b}}$ = lift coefficient based on square of dynamic beam	U = forward speed or onset freestream speed	ρ = mass density of water
$C_{L_{bl}}$ = lift coefficient based on waterplane area	v = transverse induced velocity	τ = trim angle, radians; see Fig. 1
C_D = drag coefficient based upon l^2	v_b = transverse induced velocity at waterline	φ = velocity potential function
C_f = Schoenherr flat plate drag coefficient based on area	w = vertical induced velocity	χ = defined by equation (18)
D = drag force (resistance to motion)	x, y, z = longitudinal, transverse, vertical coordinates; see Fig. 1	ψ = equations (12) and (13)
D_{nv}, D_f = nonviscous drag; skin friction drag	z_{hc}, z_h = vertical ordinate of families of hull surface	$\Gamma(x)$ = Euler gamma function
D_s = drag arising from generation of spray		θ = equation (12)
	Greek	
	α_0 = semi-apex angle of static waterplane	
	α = semi-apex angle of dynamic waterplane	
	α_b = angle of resultant velocity at waterline	

was the inclusion of the component of induced transverse velocity normal to the hull and removal of the singular behavior at the spray root by an elaborate extension of Tulin's (1957) procedure. Vorus thereby obtained an integral equation of the second kind in lieu of one of the first kind which arose in Wagner's (1932) model. The Vorus model is complicated by accommodating varying cross-section shapes. His theory provides the essential input for steady-state planing of slender hulls of moderate deadrise. To date Vorus has not published applications to planing although he has promised to do so.

The first experimenter to investigate the influences of camber appears to be John Plum, a Danish yachtsman-intuitive naval architect who was granted a patent on his "Fantail" design. In the late 1920's he built a 35-ft (10.7 m) boat which involved a stepped hull with camber forward and an adjustable stabilizer aft. In this way he reduced the wetted surface while providing trim control. While at the David Taylor Model Basin he influenced a young graduate naval architect, Eugene Clement, who furthered the concept by conducting model experiments with cambered surfaces and models of stepped hulls—a short cambered surface with deadrise extending forward of the step and the Plum "Fantail" stabilizer aft—while exploiting the depressed water surface aft of the step to provide a dry afterbody. This design thus eliminates the inefficient wetted area of the afterbody and has been shown to reduce total resistance remarkably. Later Clement replaced the stabilizer by twin hydrofoils at the stern. The experiments on cambered surfaces of zero deadrise by Moore (1967) showed lift/drag ratios of 15 compared with about 8 for the same area and lift. This work and the summary of Clement & Koelbel (1992) has inspired this current effort.

In the 1930's Sottorf, who conducted the first systematic series of model tests of planing forms, did a limited experimental study of circular-arc camber. He reported high lift/drag which degraded at non-optimum trim and the model displayed porpoising. These negative aspects were sufficient to convince designers and experimenters alike to drop any further consideration of cambered hulls. The introduction of trim flaps on German E-boats during WWII and their current use today on planing boats to assist in negotiating the hump resistance prior to planing is an application of effective camber, as are flaps on aircraft wings. These are set to zero flap angle at planing speed to provide optimum trim angle. To be effective, cambered hulls must provide for the center of lift to be close to the longitudinal center of mass, requiring a stepped hull with hydrofoils at the stern as pointed out by Clement.

A few other theorists have addressed planing forms with camber. Maruo (1951) analyzed planing at arbitrary Froude numbers of two-dimensional, cambered sections. Although he treated arbitrary shapes, he gave results only for flat plates. Cumberbach (1958) also produced formulas for two-dimensional shapes at high but finite Froude numbers. His singularity at the leading edge vanished at high Froude numbers, yielding elliptical loading as in airfoil theory. For a parabolic camber he found nonviscous-lift/drag ratios some eight times higher than that of a flat plate! The problem of holding viscous drag fixed by holding arc-length-to-chord constant while optimizing camber was taken up by Wu et al (1972). A pair of nonlinear integral equations when approximated by uncoupled linear equations gave results for a family of optimum shapes for a range of arc-length-to-chord. Favorable comparison with Cumberbach (1958) was noted. Although two-dimensional calculations are instructional, slender

planing forms are of low aspect ratios, with flows induced in transverse planes. Maruo (1967) has given a masterful treatment of high- and low-aspect-ratio surfaces *in the presence of gravity*. He also has identified the reduction of spray drag by camber, but again evaluated only flat surfaces. He pointed out that retention of gravity increases lift at high Froude numbers at low aspect ratios and decreases it at large aspect ratios, noting that these opposite tendencies were demonstrated previously by experiments.

Development of a mathematical model

Geometry of classes of planing surfaces

An equation of the bottom surface of a class of hulls of variable deadrise angle, $\beta(x)$, and linearly tapered camber may be written as:

$$z = z_{hc}(x, y) = y \tan \beta_c(x) - c(x) \left(1 - k \frac{y}{b(x)} \right);$$

$$k = \text{a constant: } 0 \leq k \leq 1$$

or for ease later as:

$$z = z_{hc}(x, y) = y \tan \beta_c(x) - c(x)$$

where

$$\beta_c = \tan^{-1} \left(\tan \beta(x) + k \frac{c(x)}{b(x)} \right) \quad (1)$$

A family of surfaces of varying deadrise angle without camber at trim angle, τ , is obtained by setting $k = 0$ and replacing $c(x)$ by $x \tan \tau$ to give:

$$z = z_h(x, y) = y \tan \beta(x) - x \tan \tau \quad (2)$$

For simple prismatic surfaces, β is a constant. Figure 1 displays the geometry of prismatic hulls as well as the static and dynamic half-breadths as defined by the intersections of the calm and distorted water surface with the hull. The hull is held restrained in heave and trim in a uniform flow of an inviscid fluid in which the induced motion is taken to be irrotational. All recurring symbols are defined in the Nomenclature.

The components of the unit normal of the general surface (2) are given by:

$$\vec{N} = \frac{1}{D} (F_x, F_y, F_z); F = z - z_{hc} = 0;$$

$$D = \sqrt{F_x^2 + F_y^2 + F_z^2}$$

$$F_x = -z_{hcx} = c_x - y \beta_{cx} \sec^2 \beta_c; \quad (3)$$

$$F_y = -z_{hcy} = -\tan \beta_c; \quad F_z = 1$$

$$\vec{N} = \frac{1}{D} (-z_{hcx}, -z_{hcy}, 1); D = \sqrt{z_{hcx}^2 + z_{hcy}^2 + 1}$$

Subscripts x, y, z indicate partial derivatives.

For the general class of hulls

$$\vec{N} \approx \left(\left(c_x - y \frac{\partial}{\partial x} (\tan \beta_c(x)) \right) \cos \beta_c, -\sin \beta_c, \cos \beta_c \right)$$

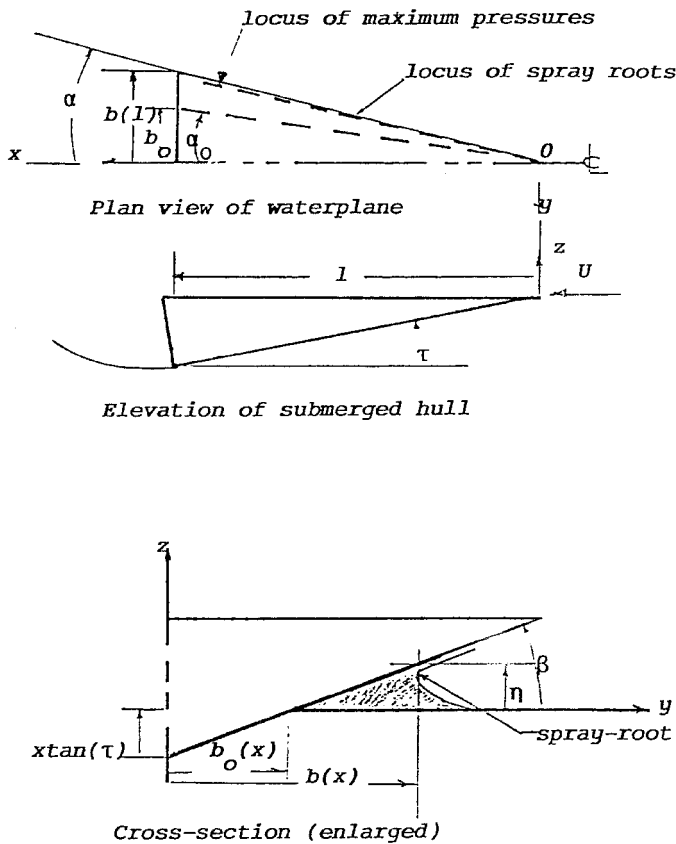


Fig. 1 Schematic of a prismatic hull defining dimensions, coordinates, and static- and dynamic half-breadths

which for prismatic forms at small trim angles, simplifies to:

$$\vec{N} \approx (\tan \tau \cos \beta, -\sin \beta, \cos \beta) \quad (4)$$

As planing craft must be slender to operate in even limited seaways, slender-body theory may be used for aspect ratios in the vicinity of unity and less. This implies that the flow is dominantly transverse except in planes very close to the bow and stern. The three-dimensional equation of continuity can be reduced to a two-dimensional one by noting that the longitudinal gradient of the x -component, $u_x(x, y, z)$ is weak for sufficiently small dynamic beam-to-length ratios thereby reducing the continuity equation to $v_y(y, z; x) + w_z(y, z; x) = 0$, in which x has the role of a parameter. This led Wagner (1932) to envision the flow in any transverse plane as that due to a descending wedge at vertical speed $U \tan \tau$. He chose to approximate this wedge flow by the flow generated by an infinitely long flat plate of expanding width at the level of the undisturbed water surface. He then found the dynamic beam by calculating the local intersection of the raised water level with the wedge-side extension. The flat-plate flow is generated by a vorticity distribution on $z = 0$ from $-b(x)$ to $+b(x)$. He found that the ratio of dynamic-to-static half-breadths was $\pi/2$, independent of the deadrise. This distinguished Wagner's theory from an earlier one of von Karman and gave much better agreements with model data. This factor has been used by empiricists and theorists alike in spite of the fact that the local

deflection of the water surface must decrease with increasing deadrise angle. The Wagner theory neglects the contribution to the normal velocity on the hull by the strong transverse induced velocity. This was noted for the first time by Vorus (1996), as stated earlier.

An approximate velocity potential

A more accurate velocity potential than those generally employed previously would consist of vorticity distributions on the boundaries of the hull cross section and its mirror image together with boundary singularities on the unknown water surface. This would involve coupled integral equations with complicated kernels for the unknown singularity strengths, forestalling any analytical progress by requiring numerical inversions. Here the distributions of vorticity are brought to the level of the calm water, yielding the simple potential:

$$\varphi(y, z; x) = \frac{1}{\pi} \int_{-a}^a \gamma(y') \tan^{-1} \left(\frac{z}{y-y'} \right) dy' \quad (5)$$

This potential and its derivatives must satisfy the following boundary conditions:

- (i) $\varphi_y(0, z_{hc}) = v(0, z_{hc}) = 0$;
- (ii) $\varphi_y(-y, z) = -\varphi_y(y, z)$
- (iii) $\vec{N} \cdot \vec{V} = 0$; $\vec{V} = (U + u, v, w)$

$$-U z_{hcx} - \varphi_y z_{hcy} + \varphi_z \approx 0; \quad U \gg \varphi_x \quad (6)$$

- (iv) $U/\sqrt{g l} \gg 1$; $\varphi(y, \eta(y; x)) = 0$; $|y| \geq a$
- (v) $\varphi_y(y, z; x) = a$ finite value for $y = b(x)$; $z = -0$

Folding the integral in (5) and dividing the limits into a large part from 0 to $b(x)$ and an assumed very small part, $(a(x) - b(x))$ gives:

$$\varphi = \frac{1}{\pi} \left\{ \int_0^b \gamma(y') K(y, y') dy' + \int_b^a \gamma(y') K(y, y') dy' \right\} \quad (7)$$

where

$$K = \left(\tan^{-1} \left[\frac{z}{y-y'} \right] - \tan^{-1} \left[\frac{z}{y+y'} \right] \right)$$

and the odd-function Condition (ii) for asymmetrical flow in y has been enforced by using $\gamma(-y') = -\gamma(y')$.

This potential does not satisfy Condition (iv) on the water surface $z = \eta(x, y)$, nor can its derivatives satisfy Condition (iii) that the total velocity normal to the hull must vanish. Applying the usual thin-section approximation, these conditions are enforced by values of the potential and all derivatives on the line $z = 0$. This implies that applications will be limited to moderate deadrise and small trim angles. Equation (7) satisfies $\varphi(y, 0; x) = 0$ for $|y| \geq a$ and yields:

$$\begin{aligned} v(y, -0; x) &= \text{Lim } \varphi_y(y, z; x)_{z \rightarrow -0} = \gamma(y); \quad |y| \leq a \\ v(y, 0; x) &= 0; \quad |y| > a \end{aligned} \quad (8)$$

These results are derived in any textbook in which the properties of singularity distributions are applied to thin sections and first-order water-wave theory, such as Newman (1977) or Breslin & Andersen (1994).

The vertical component along the y -axis is

$$w(y, 0; x) = -\frac{2}{\pi} \left\{ * \int_0^{b(x)} v(y') \left[\frac{y'}{y'^2 - y^2} \right] dy' \right. \\ \left. + v_b \int_{b(x)}^{a(x)} \left[\frac{y'}{y'^2 - y^2} \right] dy' \right\}$$

where the asterisk indicates that the integral is taken as a Cauchy principal-value integral.

Here, following Tulin on the assumption that b is very close to a , the unknown transverse velocity is virtually constant in the interval, b to a , and given by the value v_b at $y = b(x)$. After introducing the transformations, $s = y^2/b^2(x)$; $t = y'^2/b^2(x)$, the vertical induced velocity takes the following required form with Cauchy kernels:

$$w(y, 0; x) = -\frac{1}{\pi} \left\{ * \int_0^1 \frac{v(t)}{t-s} dt + v_b \int_1^{(a/b)^2} \frac{dt}{t-s} \right\}; \quad (9) \\ 0 \leq s \leq 1$$

where because $a(x)/b(x)$ is assumed very nearly 1.0, the unknown $v(t)$ in the last integral is taken to be constant and defined as v_b , the value of the unknown transverse velocity v at the waterline. There are now four unknowns, viz., $v(s)$, a/b , v_b and $b(x)$; $v(s)$ will be found as a functional of the other three from the inversion of an integral equation; a/b to meet Condition (v), finiteness of $v(b(x))$; v_b by requiring the pressure to the atmospheric at $y = b$; and finally $b(x)$ is determined from solving for the intersection of the deflected water surface with the extended hull.

Determination of the unknown functions

The transverse velocity $v(y, 0; x)$

Enforcement of Condition (iii) that the total normal component at the hull yields the following constraint on $v(y, 0; x)$:

$$(z_{hcy})v(s) + \frac{1}{\pi} * \int_0^1 \frac{v(t)}{t-s} dt \\ = (-z_{hcx})U - \frac{1}{\pi} v_b \int_1^{(a/b)^2} \frac{1}{t-s} dt; \quad (10) \\ \text{for } 0 \leq s \leq 1$$

Equation (10) is a Cauchy, inhomogeneous integral equation of the second kind for $v(s) = v(y^2/b^2)$. Fortunately, equations of this type were inverted by Carleman (1923) as well as the equation of the first kind, which is better known because it arises in airfoil theory. It is the presence of $v(s)$ in (10) which classifies the equation as that of the second kind. When this term is not included and the last term on the right-hand side (rhs) of (10) is omitted, equation (10) reduces to that of Wagner (1932) which gives singular $v(b)$ and dynamic-to-static half-breadth ratio of $\pi/2$. The inclusion of the contribution of the transverse component to the normal velocity on the hull was introduced by Vorus (1996) as well as a more elaborate procedure to yield finite velocity at $y = b(x)$.

As may be gleaned (with difficulty!) from Tricomi (1957), integral equations of the following form,

$$\psi(s)v(s) - \lambda \int_{-1}^1 \frac{v(t)}{t-s} dt = f(s) \quad (11)$$

have the following inversion:

$$v = \frac{\psi(s)f(s)}{\psi^2 + (\pi\lambda)^2} + \frac{\lambda e^\theta}{(1-s)\sqrt{\psi^2 + (\pi\lambda)^2}} \\ * \int_{-1}^1 \frac{(1-t)f(t)e^{-\theta(t)}}{\sqrt{\psi^2 + (\pi\lambda)^2}(t-s)} dt + \frac{C e^{\theta(s)}}{(1-s)\sqrt{\psi^2 + (\pi\lambda)^2}}; \\ \theta(s) = \frac{1}{\pi} * \int_{-1}^1 \vartheta(t') \frac{dt'}{(t'-s)}; \vartheta = \tan^{-1} \left(\frac{\pi\lambda}{\psi(t')} \right) \quad (12) \\ \vartheta = \tan^{-1} \left(\frac{\pi\lambda}{\psi(t')} \right); \lambda > 0 \\ = \pi - \tan^{-1} \left(\frac{\pi|\lambda|}{\psi(t')} \right); \lambda < 0$$

where C is a constant.

The constant C is determined by satisfying one endpoint condition, leaving v normally infinite at the other. Here that singularity will be avoided, giving a finite $v(b)$.

It is clear that for equations of the form of (11) in which the coefficient of v is a function of s (or y) the solution is complicated. This is the reason for limiting the camber to a linear function of y since in the case herein ψ is the y -derivative of the surface and hence is a constant.

For ψ independent of s , equation (12) simplifies to:

$$v = \frac{1}{\psi^2 + (\pi\lambda)^2} \left\{ \psi f + \frac{\lambda e^\theta}{1-s} \int_{-1}^1 \frac{(1-t)f(t)e^{-\theta(t)}}{t-s} dt \right\} \\ + \frac{C e^{\theta(s)}}{(1-s)\sqrt{\psi^2 + (\pi\lambda)^2}} \quad (13)$$

where the t -integral is a principal-value integral. Hereafter the asterisk will be generally omitted for ease of transcription.

Comparing with (10) and using (1), the functions in (13) are (for the most general class of hulls considered here):

$$\psi = \tan \beta_c(x); \quad \lambda = -\frac{1}{\pi}; \\ f = U(c(x) - m(x)\sqrt{s}) - \frac{v_b}{\pi} \int_1^{(a/b)^2} \frac{1}{t-s} dt; \\ m(x) = b(x)(\beta_c)_x \sec^2 \beta_c; \\ \theta(s) = \frac{1}{\pi} * \int_0^1 \frac{(\pi - \tan^{-1}(\cot \beta_c))}{t-s} dt \\ \theta = \frac{1}{\pi} * \int_0^1 \frac{(\pi - \tan^{-1}(\tan(\pi/2 - \beta_c)))}{t-s} dt \\ = \left(\frac{1}{2} - \frac{\beta_c}{\pi} \right) \ln \left[\frac{1-s}{s} \right] \\ e^{\theta(s)} = \left(\frac{1-s}{s} \right)^{\left(\frac{1}{2} - \frac{\beta_c}{\pi} \right)}$$

With the foregoing as input (13) takes the form:

$$v = \left\{ f \tan \beta_c - \frac{1}{\pi K_1(s)} \int_0^1 \frac{K_1(t)}{t-s} f(t) dt \right\} \cos^2 \beta_c + \frac{C \cos \beta_c}{s^{1/2+\beta_c/\pi}(1-s)^{1/2-\beta_c/\pi}} \quad (14)$$

where

$$K_1 = s^{1/2+\beta_c/\pi}(1-s)^\mu$$

Enforcing Condition (i), $(v(0,0;x) = 0)$ determines C by multiplying by s and by taking the limit as $s \rightarrow 0$. This yields

$$v = \left\{ f \tan \beta_c - \frac{U}{\pi} \left(\frac{s}{1-s} \right)^\mu \times \left(c_x i_1 - m(x) i_2 - \frac{v_b}{\pi} i_3 \right) \right\} \cos^2 \beta_c$$

where the i_n are

$$i_1 = \int_0^1 \left(\frac{1-t}{t} \right)^\mu \frac{dt}{t-s} = \pi \left(\frac{1-s}{s} \right)^\mu \tan \beta_c - \pi \sec \beta_c;$$

$$\text{with } \mu = \frac{1}{2} - \frac{\beta_c}{\pi};$$

$$i_2 = \int_0^1 \frac{(1-t)}{(t-s)} \frac{t^{\beta_c/\pi} dt}{(1-t)^{1/2+\beta_c/\pi}} = \pi s^{\beta_c/\pi} (1-s)^\mu \tan \beta_c - \frac{2}{\sqrt{\pi}} \Gamma \left(1 + \frac{\beta_c}{\pi} \right) \Gamma(\mu)$$

$$i_3 = \int_1^{(a/b)^2} \frac{1}{\xi-s} \int_0^1 \left(\frac{1}{t-s} + \frac{1}{\xi-t} \right) \times \left(\frac{1-t}{t} \right)^\mu dt d\xi \quad (15)$$

$$= -\pi \left(\frac{1-s}{s} \right)^\mu \int_1^{(a/b)^2} \frac{d\xi}{\xi-s} \tan \beta_c - \pi \int_1^{(a/b)^2} \left(\frac{\xi-1}{\xi} \right)^\mu \frac{d\xi}{\xi-s} \sec \beta_c$$

where Γ is the Euler gamma function and only the t -integral in the double integral is a Cauchy principal-value integral as $0 < s < 1$.

Integrals of these Cauchy types with branch points and poles within and beyond the limits are included, for example, in Gradshteyn & Ryzhik (1985) (hereafter G&R), page 290, #3.228-3. However because of the generality of the integrands, their results frequently contain hypergeometric functions which may or may not have simple equivalents not easily recognizable. The following results are given by contour integrations for those terms involving poles and branch points. (Worthy exercises for interested students!)

Upon insertion of these results into (14), the term $f(s)c_x(x)$ is annulled by the residues of poles, leaving:

$$v = \left(\frac{s}{1-s} \right)^\mu \times \left\{ U c_x(x) + \frac{v_b}{\pi} \int_1^{(a/b)^2} \left(\frac{\xi-1}{\xi} \right)^\mu \frac{d\xi}{\xi-s} - \frac{2}{\pi^{3/2}} m(x) \Gamma \left(1 + \frac{\beta_c}{\pi} \right) \cos \beta_c \right\} \cos \beta_c \quad (16)$$

The remaining integral is reduced by the substitution $q^2 = \xi - 1$ to give:

$$v = \left\{ \left(\frac{s}{1-s} \right)^\mu \left(-\frac{v_b}{\pi \mu} (2\varepsilon)^\mu - 2m(x) H(\beta_c(x)) + U c_x \right) + \frac{2}{\pi} v_b s^\mu (1-s)^\nu \int_0^{\sqrt{2\varepsilon}} \frac{q^{-2\beta_c/\pi}}{q^2 + (1-s)} dq \right\} \cos \beta_c \quad (17)$$

$$\text{where } \mu = \frac{1}{2} - \frac{\beta_c}{\pi}; v = \frac{1}{2} + \frac{\beta_c}{\pi}; \varepsilon = \frac{(a(x) - b(x))}{b(x)}; H = \frac{2}{\pi^{3/2}} \Gamma \left(1 + \frac{\beta_c}{\pi} \right) \Gamma(\mu) \cos \beta_c$$

In the above-cited transformation of the integral, the upper limit becomes $(a^2 - b^2)/b^2 = (a-b)(a+b)/b^2 \cong 2(a-b)/b$, for $a \approx b$, and $1 + q^2$ is replaced by 1 since $\sqrt{2\varepsilon} \ll 1$, which will be shown later.

Determination of epsilon

It is apparent in (17) that the first term within the braces is singular while the last term is regular at $s = 1$. Consequently for regularity required by Condition (v) the first term must vanish, forcing the following requirement on $\sqrt{2\varepsilon}$:

$$\sqrt{2\varepsilon} = \chi^{1/2\mu} \quad (18)$$

$$\chi = \left\{ \pi \mu \frac{U}{v_b} (c_x - m(x) H \cos \beta_c) \right\}$$

The transverse velocity is now given by

$$v = \frac{2}{\pi} v_b s^\mu (1-s)^\nu \int_0^{\sqrt{2\varepsilon}} \frac{q^{-2\beta_c/\pi}}{q^2 + (1-s)} dq \cos \beta_c(x) \quad (19)$$

$$\text{with } v = \frac{1}{2} + \frac{\beta_c}{\pi}.$$

Here v is seen to vanish at the keel and appears to vanish at $s = 1$, which cannot be. To show that $v(b,0;x) = v_b$, the substitution $q = \sqrt{1-s} \tan q'$ converts (19) to:

$$v = \frac{2}{\pi} v_b s^\mu \int_0^{q_1} dq' (\tan q')^{-2\beta_c/\pi} \cos \beta_c \quad (20)$$

$$\text{with } q_1 = \tan^{-1} \left(\sqrt{\frac{2\varepsilon}{1-s}} \right)$$

Taking the limit for $s = 1$, the integral yields $\frac{\pi}{2} \sec \beta_c$, (G&R p. 369, #3.622,2), whence v at $y = b$ is v_b as defined.

The q -integral can be converted to a form by the transformation $q = \sqrt{2\epsilon t}$ to give:

$$(2\epsilon)^\mu \int_0^1 \frac{t^{-2\beta_c/\pi}}{1-s+2\epsilon t} dt = \left[\frac{(2\epsilon)^\mu}{2\mu(1-s)} \right] {}_2F_1 \left[1, \mu; 1+\mu; \frac{2\epsilon}{s-1} \right] \quad (21)$$

where ${}_2F_1$ is a Hypergeometric function. (This result is given by MATHEMATICA (3.0); the t -integral does not appear to be given by G&R.)

With (21), equation (19) becomes:

$$v = \frac{v_b(2\epsilon)^\mu}{\pi\mu} \left(\frac{s}{1-s} \right)^\mu {}_2F_1 \left(1, \mu; 1+\mu; \frac{2\epsilon}{s-1} \right) \cos \beta_c \quad (22)$$

An extremely accurate approximation to (22), suitable for use in integrations, is given by the first term in the series for the Hypergeometric function, which leaves

$$v \cong \frac{v_b(2\epsilon)^\mu}{\pi\mu} \left(\frac{s}{1-s} \right)^\mu \cos \beta_c \quad (23)$$

The singularity at $s = 1$ is integrable as well as the square of $v(b(x)!$ This is in marked contrast to the limit of the Wagner exterior solution, which omits the dependence on the deadrise angle and produces infinite nonlinear pressure at the spray root. Integrability and the closeness to (22) (to be shown below) allows continued analytical formulas to be developed by using (23).

Determination of $v(b(x), 0; x)$

The consistent form of the Bernoulli equation in slender-body theory is

$$p/\rho = -Uu - \frac{1}{2}v^2 \quad (24)$$

in which p is the change in pressure from ambient.

Along the spray root, $p = 0$, hence

$$v_b^2 = -2U \frac{\partial}{\partial x} \left\{ \frac{1}{\pi} \int_0^{b(x)} v \left[\tan^{-1} \left(\frac{z}{y-y'} \right) - \tan^{-1} \left(\frac{z}{y+y'} \right) \right]_{z \rightarrow 0} dy' \right\}$$

The angle subtended by the first arctangent is 0 for $y > y'$ and $-\pi$ for $y < y'$. The last term gives zero, leaving

$$v_b^2 = 2U b_x(x) v_b \quad \text{whence} \quad (25)$$

$$v_b = 2U b_x(x); v_b = 0$$

The transverse velocity is seen to vary as the slope of the dynamic waterline, and v is now

$$v = \frac{2b_x U (2\epsilon)^\mu}{\pi\mu} \left(\frac{s}{1-s} \right)^\mu {}_2F_1 \left(1, \mu; 1+\mu; \frac{2\epsilon}{s-1} \right) \cos \beta_c \quad (26)$$

and

$$v \cong \frac{2b_x U (2\epsilon)^\mu}{\pi\mu} \left(\frac{s}{1-s} \right) \cos \beta_c \quad (27)$$

Recalling that the dynamic half-breadth, $b(x)$, is still unknown, v is not yet determined. As $b(x)$ is dependent upon the shape of the hull, it is necessary to treat each hull class separately.

Classes of hulls

Class I: prismatic

Prismatic hulls are of constant deadrise angle without camber. The static half-breadth is simply obtained from the general class by taking $c(x) = x \tan \tau$; $\beta_c = \beta$ and $k = 0$. The static half-breadth is

$$b_0(x) = x \frac{\tan \tau}{\tan \beta} \quad \text{and} \quad 2\epsilon = \left(\pi\mu \frac{U}{v_b} \tan \tau \right)^{\frac{1}{\mu}} \quad (28)$$

Then (23) is reduced to

$$\frac{v}{U} \cong \left(\frac{s}{1-s} \right)^\mu \tan \tau \cos \beta; \quad \mu = \frac{1}{2} - \frac{\beta}{\pi} \quad (29)$$

The kinematical condition on the water surface is (for $U \gg u$)

$$-U\eta_x - v\eta_y + w = 0; \quad \text{for } 1 < s < \infty$$

As $v = 0$ for $s > 1$ and w is nonzero only in way of the waterplane, upon integrating, the water surface deflection along fixed y to any x intersecting the waterline, assuming $\eta(y; 0) = 0$, one has

$$\eta = \frac{1}{U} \int_0^x w(s, 0; x') dx' \quad (30)$$

where w is to be found from

$$w(y, 0; x) = -\frac{1}{\pi} \int_0^1 \frac{v(t)}{t-s} dt - \frac{v_b}{\pi} * \int_1^{(1+\epsilon)^2} \frac{dt}{t-s};$$

for $s \geq 1s \geq 1$

The last term is negligible because of the very smallness of ϵ (to be shown after $b(x)$ is found). Using (29) in place of the exact expression for v yields

$$w(y, 0; x) = U \left(\left(\frac{y^2}{y^2 - b^2(x)} \right)^\mu - 1 \right) \tan \tau \quad (31)$$

Insertion of (30) into (29) results in:

$$\eta(y; x) + x \tan \tau = \eta^*(y; x) = y^{2\mu} \int_0^x \frac{dx'}{(y^2 - b^2(x'))^\mu} \tan \tau$$

where from the hull geometry η^* is the height of the water surface above the keel at any y in way of the hull, as may be seen in Fig. 1. For $y = b(x)$, $\eta^* b(x) = b(x) \tan \beta$ and then

$$b(x) \tan \beta = \int_0^x \left(\frac{b^2(x)}{b^2(x) - b^2(x')} \right)^\mu dx' \tan \tau \quad (32)$$

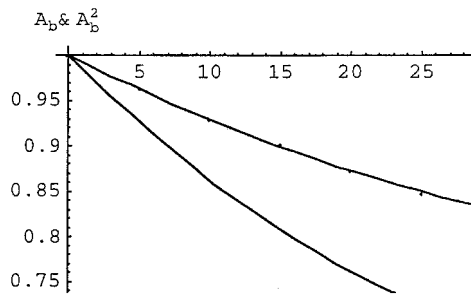


Fig. 2 Variation of attenuation coefficient A_b as defined by equation (34) or (34a) and its square with deadrise angle

Substituting

$$b(x') = b(x)\sqrt{\lambda}; dx' = \frac{dx'}{db(x')} db(x') = \frac{b(x)}{b(x')} \frac{d\lambda}{2\sqrt{\lambda}}$$

and noting that at $x' = x$, the integration over all dummy $b(x')$ has an upper limit of $b(x)$, (32) is reduced to:

$$\tan \beta = \frac{1}{2} \int_0^1 \frac{1}{b_x} \lambda^{-\frac{1}{2}} (1-\lambda)^{-\frac{1}{2} + \frac{\beta}{\pi}} \tan \tau \quad (33)$$

Model experiments have shown waterplanes in way of the chines-dry region to be very nearly triangular; consequently the slope of the waterline is taken to be constant so $b_{x'} = b_x$ may be passed through the integral. Then the integral is recognized as a Beta function, which can be converted to a product of Gamma functions to give finally

$$b(x) = \frac{\pi}{2} A_b b_0(x) \quad (34)$$

where $A_b = \left(\frac{1}{\sqrt{\pi}} \frac{\Gamma(1/2 + \beta/\pi)}{\Gamma(1 + \beta/\pi)} \right)$; $b_0 = x \frac{\tan \tau}{\tan \beta}$

A_b is defined to be an attenuation coefficient of the half-breadths as deadrise angle is increased. It is unity for zero deadrise, showing that the constant Wagnerian factor, $\pi/2$ is correct only for vanishing β .

Figure 2 shows that this attenuation coefficient is definitely significant and especially its square, which arises in expressions for lift and drag. More readily applicable forms for A_b and A_b^2 are provided by their following least-squares very close fits:

$$\begin{aligned} A_b &= 1 - 0.007957\beta + 0.0007714\beta^2; \\ A_b^2 &= 1 - 0.01591\beta + 0.0002176\beta^2 \end{aligned} \quad (34a)$$

Here β is in degrees.

A comparison with Vorus's (1996) corresponding factor, J , as given in his Table (2a) is displayed in Table 1, showing very close agreement. Differences are due to his use of $\sin \beta$ rather than $\tan \beta$ in his kinematical condition.

Justifications of approximations and limitations of theory

It has been assumed that ε is very small. As $b(x)$ is now known, this may be verified. From the foregoing equation (28), it

Table 1 Comparison of attenuation factor, with Vorus's wetting factor for three values of deadrise angles

β	10	20	30
A_b	0.929	0.872	0.83
J	0.929	0.874	0.834
A_b^2	0.863	0.760	0.692
J^2	0.863	0.764	0.696

may now be expressed by:

$$\varepsilon = \frac{1}{2} \left[\frac{\sqrt{\pi} \mu \Gamma(1 + \beta/\pi)}{2\Gamma(1/2 + \beta/\pi)} \tan \beta \right]^{\frac{1}{\mu}}; \mu = \frac{1}{2} - \frac{\beta}{\pi} \quad (35)$$

A graph of ε in Fig. 3 shows that it is extremely smaller than 1.0 over the entire range of applicable deadrise angles. This is consonant with the assumptions in the foregoing.

The expressions for the exact and approximate formulas (26) and (27) become with (35), for this hull class, simply

$$\frac{v}{U} = \left(\frac{s}{1-s} \right)^{\mu} {}_2F_1 \left(1, \mu; 1 + \mu; \frac{2\varepsilon}{s-1} \right) \cos \beta \tan \tau \quad (36)$$

$$\frac{v}{U} \cong \left(\frac{s}{1-s} \right)^{\mu} \cos \beta \tan \tau; \mu = \frac{1}{2} - \frac{\beta}{\pi} \quad (37)$$

The validity for use in integrations of the approximation (37) for the transverse velocity in lieu of the exact expression, (36), is shown by the list of the ratio of the exact-to-approximate v/v_{app} , displayed in Table 2. The approximation is excellent up to $s = 0.98$, or $y = 0.99b(x)$. The exact $(v \cot \tau)/U = 4.53$ at $y = b(x)$ and $\beta = 30$ deg, whereas (37) is infinite. Of course, for calculation of v and pressure in the very near vicinity of the waterline (where they are greatest), one must use equation (36).

It is very important to recognize that slender-body theory cannot accommodate all combinations of trim and deadrise angles. To define a domain of permissible trim angles for a range of deadrise from, say 0 to 40 deg, one may expect to require that the aspect ratio of the dynamic waterplane be limited to a maximum of 1.0. This is because of the failure of low-aspect-ratio wing theory to predict lift of delta wings much beyond an aspect ratio of unity. With this presumption, the following is taken as a

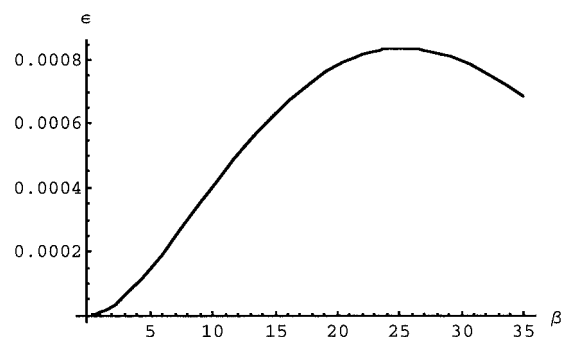


Fig. 3 Variation of parameter ε , with β defined by equation (35)

Table 2 Ratio of exact to approximate transverse velocities for various values of $(y/b(x))$

	0	0.2	0.4	0.6	0.8	0.9	0.99
	1.00	0.997	0.994	0.992	0.985	0.971	0.479

bound for trims of triangular waterplanes:

$$\tau \leq \tan^{-1} \left(\frac{\Gamma(1 + \beta/\pi)}{2\sqrt{\pi}\Gamma(1/2 + \beta/\pi)} \right) \quad (38)$$

The region below this bound is displayed in Fig. 4. This criterion is seen to be too conservative relative to correlations with measurements of wetted length and beam of prismatic forms in the chines-dry mode shown below.

Correlations with model data

Waterplane semi-apex angle

The semi-apex angle of waterlines as a function of trim and deadrise angles is given by

$$\alpha = \tan^{-1} \left(\frac{\sqrt{\pi}\Gamma(1/2 + \beta/\pi)\tan\tau}{2\Gamma(1 + \beta/\pi)\tan\beta} \right) \quad (39)$$

Equation (39) is graphed in Fig. 5 for three values of trim over the range of deadrise angles for which measurements of wetted beam and lengths were made by Pierson et al (1954). These data points are superposed with the aspect ratio of each waterplane. It is clear that although the correlations at $\beta = 10$ deg are not as good as the remarkable ones at 20 and 30 deg, the near agreements are acceptable despite the relatively large aspect ratios. The criterion of unit aspect ratio requires that the semi-apex angle not exceed 14 deg! For this aspect of the flow pattern it appears that restriction to unit aspect ratio is too conservative.

Transverse velocity at waterline

The expression for the transverse velocity at the spray root, $y = b(x)$, can now be found for this class of hulls as $b(x)$ has been determined. It is

$$v_b = 2Ub_x = 2U \tan \alpha$$

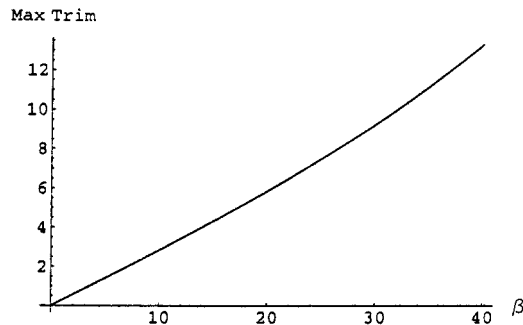


Fig. 4 Limit of permissible trim angles as a function of deadrise angle for waterplanes of unit aspect ratio given by equation (38)

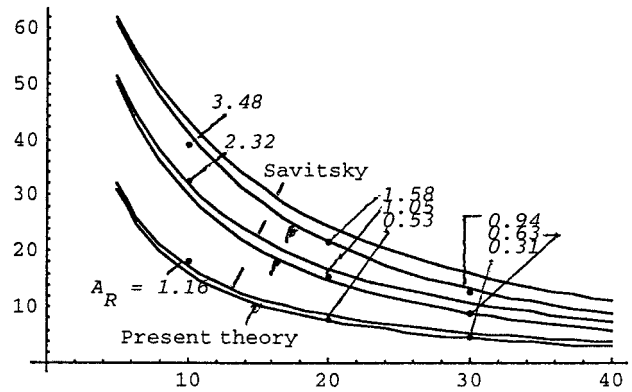


Fig. 5 Comparison of semi-apex angles given by the present theory (equation (39)) with derived values from data of Pierson et al (1954) and the theory in Savitsky (1964) at trim angles of 2, 4, and 6 degs over test range of deadrise angles

The angle from the centerline of the resultant flow at the waterline (of magnitude $V = \sqrt{U^2 + v_b^2}$) is

$$\alpha_b = \tan^{-1} \left(\frac{v_b}{U} \right) = \tan^{-1} (2 \tan \alpha) \quad (40)$$

This compares with the approximate observations of model spray patterns that the resultant flow direction is at about twice the semi-apex angle. This is given by (40) when the tangent and its inverse may be replaced by their arguments. Figure 6 displays the flow and semi-apex angles.

Lift of prismatic hulls

Lift is usually reckoned from the gradient of added mass. This process seems to mask physical interpretation. Here it is considered to be more informative of the roles of geometric parameters to integrate the pressure distribution over the hull projection. The consistent form of Bernoulli's equation in slender-body theory is:

$$p = -\rho \left(uU + \frac{1}{2}v^2 \right)$$

The induced longitudinal component is obtained from

$$u(y, -0; x) = \frac{\partial \varphi(y, -0; x)}{\partial x} = -\frac{\partial}{\partial x} \int_y^{b(x)} v(y', 0; x) dy'$$

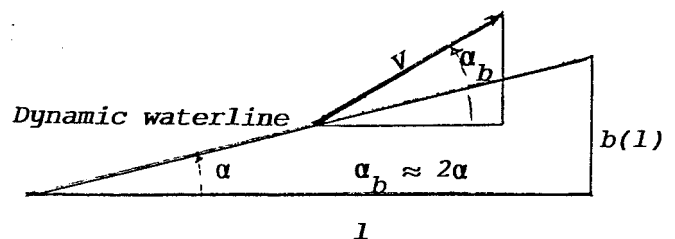


Fig. 6 Resultant flow angle at waterline from centerline equal to about twice the apex angle in agreement with many observations with models at planing speeds

The gradient of the linear part of the lift is then

$$L_x = 2\rho U \int_0^{b(x)} \frac{\partial}{\partial x} \int_y^{b(x)} v(y', 0) dy' dy$$

Interchanging orders of operation (as may be validated), integrating by parts, using the approximate form of v with $y = b(x)\sqrt{s}$, and evaluating an integral over s , yields upon integrating over x :

$$L = \pi\rho U^2 \left(\frac{1}{2} - \frac{\beta}{\pi} \right) b^2(l) (-z_{hx})|_{x=l} \quad (41)$$

It is important to note that the lift is jointly proportional to the square of the half-breadth and the slope of the hull at the stern and hence is independent of the shape of the waterplane!

This is well known by those familiar with slender, flat-wing theory as stressed by Tulin (1957). Here the new effect of additional attenuation arising from deadrise is provided by the factor $(1/2 - \beta/\pi)$ in lieu of $1/2$ as in the Wagner (1932) theory.

Defining a lift coefficient based on the square of the length (solely because the available data were so normalized) and, as for this class of hulls, $z_{hx} = -\tan \tau$ upon introducing the fit to the dynamic half-breadth:

$$C_{L_{lin}} = \frac{L}{\frac{1}{2}\rho l^2 U^2} \quad (42a)$$

$$= \frac{\pi}{2} \left(\frac{1}{2} - \frac{\beta}{180} \right) A_b^2 \tan^3 \left(\frac{\pi}{180} \tau \right) \cot^2 \left(\frac{\pi}{180} \beta \right) \quad (42b)$$

where $A_b^2 = 1 - 0.01591\beta + 0.0002176\beta^2$; β is in degrees, and (42) gives the linear part of the lift coefficient.

The total or net lift from the addition of the linear and decrement from the quadratic term in the pressure is found to be:

$$\begin{aligned} C_{L_T} = & \left\{ \frac{\pi}{2} \left(\frac{1}{2} - \frac{\beta}{180} \right) A_b^2 \right. \\ & - [(1/2 - \beta/90)\Gamma(\beta/90)\Gamma(1/2)] \\ & \times \left[\frac{\Gamma(\beta/90)\Gamma(1/2 + \beta/90) \cos^2 \left(\frac{\pi\beta}{180} \right)}{4\Gamma(1 + \beta/180) \cot \left(\frac{\pi\beta}{180} \right)} \right] \left. \right\} \\ & \times \cot^2 \left(\frac{\pi\beta}{180} \right) \tan^3 \left(\frac{\pi\tau}{180} \right) \quad (43) \end{aligned}$$

A much more preferred form of lift coefficient is that based upon the square of the *static* beam because that is the principal dimension selected by the designer. It is

$$\begin{aligned} C_{L_{2b}} = & \frac{\pi^3}{8} \left(\frac{1}{2} - \frac{\beta}{180} \right) (1 - 0.01591\beta + 0.000218\beta^2) \\ & \times \tan \frac{\pi\tau}{180}; \beta, \tau \text{ (deg)} \quad (44) \end{aligned}$$

To compare with the comparable wing, the lift coefficient is based upon the projected dynamic waterplane area to give:

$$C_{L_{bl}} = \frac{\pi}{2} \left(\frac{1}{2} - \frac{\beta}{180} \right) A_R \tan \frac{\pi\tau}{180} \quad (45)$$

where $A_R = \frac{4b(l)}{l}$ is the dynamic aspect ratio.

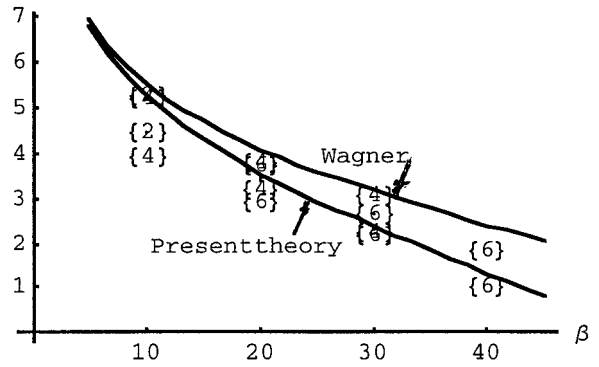


Fig. 7 Correlations of natural logarithms of the normalized theoretical-linear and experimental lift coefficients, $\ln(C_L \cot^3 \tau)$, with bounds of data points given in Pierson et al (1954) from measurements other than theirs. It is clear that the Wagner theory overestimates all bounds

The limit of (42b) as $\beta \rightarrow 0$ is just half of the well-known value of the aerodynamicist's result for triangular wings. *This is a necessary condition for the foregoing development to be correct.* This is also the required limit for slender waterplanes of small semi-apex angles rather than the rectangular flat-plate limit used to develop empirical formulas as in Savitsky (1964).

Natural logarithms of normalized lift coefficients defined as $C_{L_{lin}} \cot^3 \tau$ and $C_L \cot^3 \tau$ from (42) and (43) are graphed in Figs. 7 and 8. In Fig. 7 the lift from the linear part of the pressure from present theory and Wagner's are compared with the indicated spreads of data at 2, 4 and 6 deg trim, showing that the Wagner formula over-estimates the upper bounds of the data. Figure 8 is restricted to the correlation of the average of measured lifts obtained by Pierson et al (1954), which data show far less scatter. Here the linear and the net-lift coefficients from the current theory show exceedingly close agreement with the deductions from model tests. It is clear that the nonlinear contribution is very small and encourages exclusion of the nonlinear aspects except when calculating pressures near the waterline.

Another "test" of the theory can be made by comparison with the Korvin-Krukovsky-Savitsky (1949) and Savitsky-Neidinger (1954) empirical fits to a broad collection of data. This work was summarized and applied by Savitsky (1964) in an available

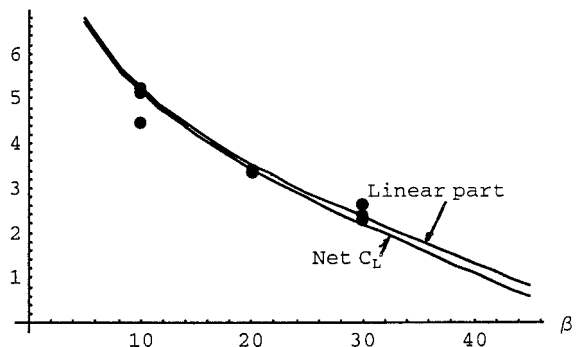


Fig. 8 Remarkable fit of the natural logarithms of linear and nonlinear normalized lift coefficients, $\ln(C_L \cot^3 \tau)$, to the consistent course of the same function of the averages of the lift coefficients derived from data obtained by Pierson et al (1954) from their model tests

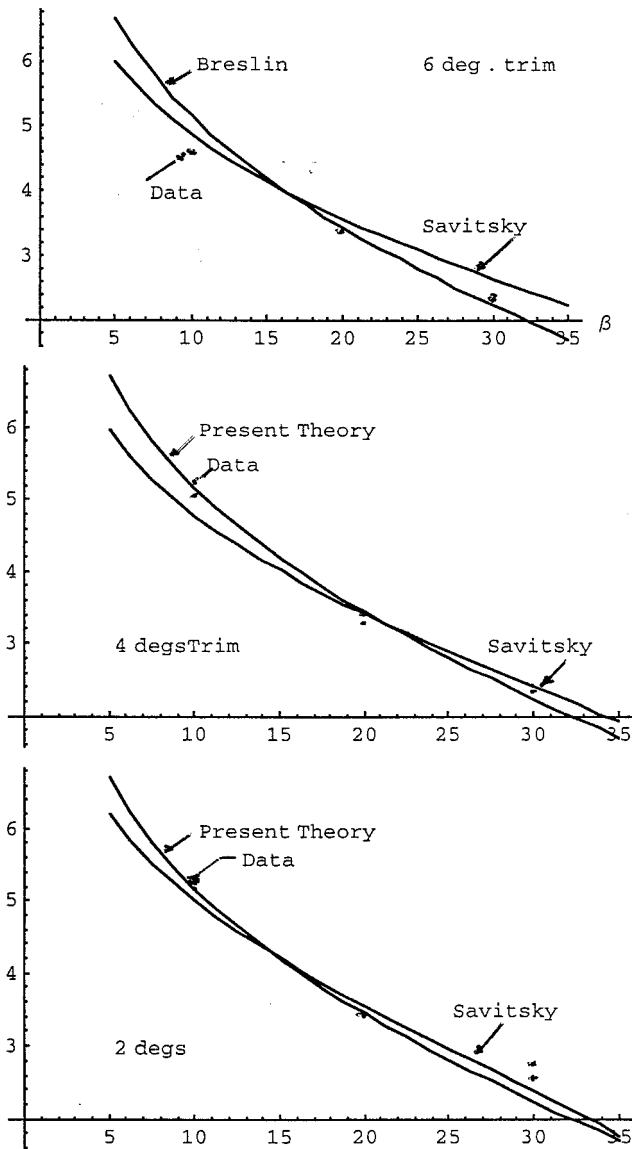


Fig. 9 Natural logarithms of normalized-lift coefficients $\ln(C_L \cot^3 \tau)$, from present theory and empirical formulations presented by Savitsky (1964) vs. deadrise angle for three trim angles

form. Figure 9 displays that the use of Savitsky's empiricism is not superior to the present theory at the important trim angle of 4 deg when compared with the data from Pierson et al (1954). He did not show in 1964 the degree to which the empirical formulas compare to the inevitable scatter of model data.

This is not intended to denigrate the cited empirical fits which cover a much broader range of hull forms and parameters than the limits inherent in slender-body theory permit. Rather, the good correlations are considered a redemption of theory which has been ignored by empiricists and pragmatic naval architects, primarily because it gave poor correlations with flat-bottomed models. But the flows about such models having apex angles of 180 deg cannot be addressed with slender-body theory! Nor did the Wagner theory work sufficiently well because of the omission of the contribution of the strong transverse flow. Moreover, the

current theory holds the promise that it may be extended to form the basis of a more rational, semi-empirical fit to existing data.

Drag of cambered and prismatic hulls

Drag has been considered as composed of that arising from the total aft component of the pressure distribution plus the viscous resistance due to shear along the bottom. This is expressed by:

$$L \tan \tau + \frac{1}{2} \rho S \bar{U}^2 C_f \quad (46)$$

with S the wetted surface; \bar{U} a mean velocity on the hull bottom and C_f is a skin friction coefficient, usually from Schoenherr, as presented by Van Manen et al (1988).

This is surely correct, foregoing any more elaborate method for the viscous part. However for slender low-aspect-ratio waterplanes at small trims (just the conditions for many planing hulls), Wagner (1932) observed that the first term above is composed of equal parts of induced drag and spray drag. While this finding does not provide drag relief for prismatic hulls, it does indicate that by application of camber and or waterline shape the spray component can be reduced. This has been reiterated by Tulin (1957), who demonstrated reductions, and by Maruo (1967) and ignored thereafter.

Consider a hull with nontapered camber ($k=0$), the nonviscous drag may be expressed as

$$D_{nv} = -2 \int_0^l dx \int_0^{b(x)} dy z_{hc} p(y, 0; x) = - \int_0^l dx z_{hc} L_x$$

and upon integrating by parts, noting that the hull slope being independent of y can be passed through the y -integral:

$$D_{nv} = (L(l)(-z_{hc})|_l - \pi \rho U^2 \mu \int_0^l \frac{\partial^2(-z_{hc})}{\partial x^2} b^2 \frac{\partial}{\partial x}(-z_{hc}(x)) dx) \quad (47)$$

Here in (47) it is clear that the nonviscous drag is dependent upon the product of the lift and the slope of the hull at the stern diminished by a functional of the product of the curvature of the camber, the slope of the camber and the square of the half-breadth. Assuming that the first term is the induced drag of the comparable dihedral wing, then, following Wagner, half of it is the induced drag of the hull and hence the spray drag is given by

$$D_s = \frac{1}{2} L(l)(-z_{hc})|_l - \pi \rho \mu U^2 \int_0^l z_{hc} b^2(x) dx \quad (48)$$

As the induced drag cannot be reduced for any nonzero lift, (48) shows that the reduction of drag by camber is bounded by the first term, or the induced drag.

Limiting now to the class of prismatic forms for which there are experimental data, the total drag/lift ratio is

$$\frac{D_T}{L} = \tan \tau + \frac{C_f \Gamma(1/2 + \nu) \bar{U}^2}{\pi^{3/2} \mu \Gamma(\nu) \tan^2 \tau U^2} \sec \beta \tan \beta \quad (49)$$

with

$$\begin{aligned} \mu &= 1/2 - \beta/\pi; \nu = 1/2 + \beta/\pi \\ \frac{\bar{U}}{U} &= 1 - \frac{\sqrt{\pi} \mu \Gamma(\nu) \tan^2 \tau}{2 \Gamma(1/2 + \nu) \tan \beta} \end{aligned}$$

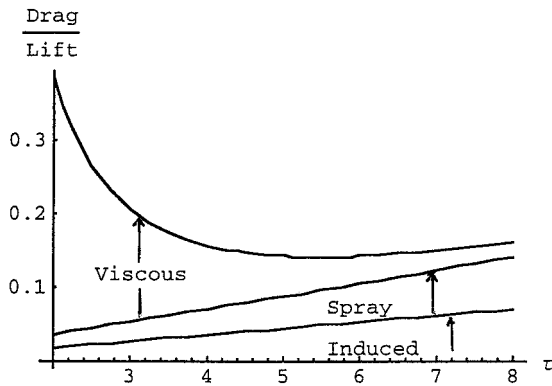


Fig. 10 Components of drag/lift ratio showing the contributions of induced spray and viscous drags at 20 deg of deadrise as a function of trim angle

Equation (49) results from the use of (34) and (41).

Figure 10 displays the various components of the drag/lift ratio for a deadrise angle of 20 deg, showing the relative contributions of induced, spray, and skin-friction drags as a function of trim angle at a Reynolds number of 2.9 million, at which the Schoenherr frictional-resistance coefficient is 0.0037 for a model with a wetted keel length of 2.0 ft (0.61 m). For the prototype craft at 35 ft (10.7 m), the optimum D/L would be some 13% less, because of the decrease in frictional resistance coefficient with increase of Reynolds number. The significance of the course of the total drag/lift curve with trim angle is that the minimum is at about 5.5 deg, in consonance with model test experience for this deadrise angle. Figure 11 shows the degradation of L/D with increase of deadrise angle from 5 to 20 deg as well as the migration of the angle of optimum performance.

Pressure distribution and center of lift

Pressure—Hull bottom pressure is taken to be that on the underside of the line of vorticity in $0 < y < b(x)$. In terms of the usual pressure coefficient:

$$C_p(y, -0; x) = \frac{p(y, -0; x)}{\rho U^2/2} = -2 \frac{u(y, -0; x)}{U} - \left(\frac{v(y, -0; x)}{U} \right)^2 \quad (50)$$

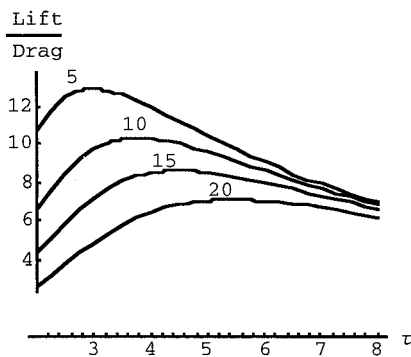


Fig. 11 Degradation of lift/drag ratio with increasing deadrise from 5 to 20 deg and migration of the optimum trim angle

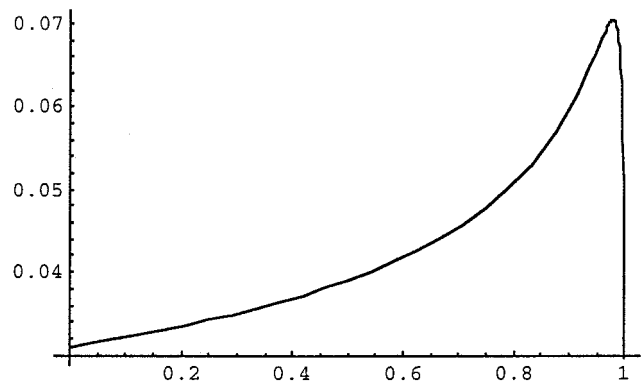


Fig. 12 Variation of pressure coefficient C_p (defined in (50)) at 20 deg deadrise and 4 deg trim with dimensionless athwartship parameter, s . Maximum C_p is about 0.070 far below 1.0 for stagnation pressure and it is located just inboard of the locus of the spray root, as has been observed in model tests

The longitudinal component, u , is given by

$$u = -\frac{\partial}{\partial x} \int_y^{b(x)} v \left(\frac{y'^2}{b^2} \right) dy'$$

and by differentiating, using the prior change of variable, yields

$$u(s) = -b_x \left\{ \sqrt{s} v(s) + \frac{1}{2} \int_s^1 dt t^{\mu-1/2} (1-t)^{\nu-1} \cos \beta \tan \tau \right\} \quad (51)$$

The t -integral can be written as a Beta function diminished by an incomplete beta function for which, fortunately, an identity exists in terms of a hypergeometric function.

The pressure coefficient reduces to

$$\frac{C_p}{\tan^2 \tau} = \left\{ \begin{array}{l} \frac{\pi}{2} A_b \left(\frac{s^{\mu+1/2}}{(1-s)^\mu} {}_2F_1 \left(1, \mu; 1 + \mu; \frac{2\varepsilon}{1-s} \right) \right) \\ + \frac{1}{2} \left\{ \frac{\Gamma(\mu+1/2)\Gamma(\nu)}{\Gamma(3/2)} - \frac{s^{1/2+\mu}}{\mu+1/2} {}_2F_1 \left(1/2 + \mu; 1 - \nu; s \right) \right\} \frac{\cos \beta}{\tan \beta} \\ - \frac{s^{1/2+\mu}}{\mu+1/2} {}_2F_1 \left(1/2 + \mu; 1 - \nu; s \right) \frac{\cos \beta}{\tan \beta} \\ - \left\{ \left(\frac{s}{1-s} \right)^\mu {}_2F_1 \left(1, \mu; 1 + \mu; \frac{2\varepsilon}{s-1} \right) \right\}^2 \cos^2 \beta \end{array} \right\} \quad (52)$$

where the reduced form of (26) has been used for v and $2\varepsilon = (\mu \tan \beta / A_b)^{1/\mu}$.

Evaluation of C_p for $\beta = 20$ and $\tau = 4$ deg is shown in Fig. 12, where it is clear that the peak pressure, 0.07, is *extremely close to the spray root (at $0.988b(x)$) as has been observed experimentally*. It is also clear that this pressure is far below stagnation pressure. The practice of referring to the loci of maximum pressure as “stagnation lines” is surely misleading.

Faltinsen (F) at the Department of Marine Hydrodynamics, Norwegian University of Science and Technology, and Zhao (Z) at Marintek A/S Trondheim, have conducted extensive studies of vertical impact of wedges on water, reported in several landmark papers. In Z&F (1993), they have applied boundary-element methods to model wedges of arbitrary shape by use of singularities on the wedge and along the level of the calm-water surface

to account for the distortion during entry while retaining nonlinear terms. They displayed close correlations of pressure distributions and the spray geometry with their extensive evaluations of an exact modeling by Dobrovol'skaya (1969). Good agreement was also achieved at small trim angles with a theory employing Wagner's (1932) local jet flow analysis together with Cointe's (1991) matched asymptotic procedure.

Figure 13 shows a comparison at 20 deg deadrise of normalized pressure coefficients (as defined by equation (47)) from the present theory, from Z&F (1993) (by curve-fitting values from their Fig. (6e 1)) and the result from present theory, labeled "Wagner" by setting $\mu = \nu = 1/2$. Z&F majorize the present curve while following closely to the "Wagner" curve. Application of their theory to planing when compared with the data of Pierson et al (1954) will overestimate lift and waterplane geometry.

Indeed, in Zhao et al (1997), their theory compared with Savitsky's (1964) empirical fit showed 33% higher lift at 4 deg trim and 20 deg deadrise and a mean wetted-length/beam ratio of unity (aspect ratio = 1 for a triangular waterplane) and substantial overestimates at all other ratios (lower aspect ratios). These differences were ascribed to three-dimensional effects. However, similar theory for low aspect wings has shown good comparison with experimental lifts up to an aspect ratio of about 1.0. Because the lift of comparable planing areas is one-half that of wings for the small, practical trim angles used, it seems doubtful that 3-D effects are present except very near the bow and step or stern for beam/lengths less than 1/2. It seems sufficient to define the waterplane half-breadths, $b(x)$, by the offsets of the spray root where the pressure is virtually atmospheric. Z&F (1993) show no drop in the ratio of dynamic to static half-breadths with increasing deadrise angle, being always the Wagner value of $\pi/2$, while Zhao et al (1997) have given falling values in their hull "half-breadths" (defined by the points at which the tapered spray vanishes on the hull and where the pressure is taken to vanish). This is outboard of the spray root and seems to have no practical relevance because between the offset of the spray root and the intersection the pressure is virtually zero as defined herein. It is the reduction of half-breadths of the spray root which is essential to give close correlations to the waterplane geometry and lift as determined by Pierson et al (1954) albeit for the restrictive class of chines-dry waterplanes.

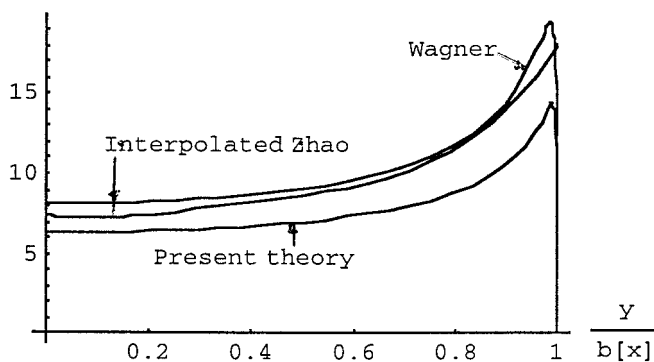


Fig. 13 Normalized-pressure coefficients, $C_p \cot^2 \tau$, from the boundary-element procedure of Zhao et al (1993); of Wagner by setting $A_b = 1$; present theory for 20 deg deadrise and 4 deg trim

Again in Zhao et al (1996) a comparison of their measured and theoretical pressures on a ship-bow model shows that their theory overestimates the experimental values. Their reference in Zhao et al (1997) to the three-dimensional lattice-based calculations of Lai (1994) which agree with the Savitsky (1964) empirical fit to data, to bolster their belief in 3-D effects, seems questionable as Lai used the half-breadths of the spray roots given by Vorus (1996) which are the same as present theory. That their several mathematical models (which indeed incorporate nearly all the physics save gravity of the induced flow, including separation at chines) do not fit the data more closely is surely surprising. The present theory, which ignores the detailed structure of the spray, may be fortuitous by compensating omissions! It should be compared with other data from good chines-dry model tests, the source of which is currently unknown.

It is of interest to compare the maximum pressure coefficients based on forward speed by replacing their drop speed, V , by $U \tan \tau$ in the criterion given by their equation (5.1), which becomes

$$C_{pMax} = 2P_{Max}/\rho U^2 = \left[\frac{\pi \tan \tau}{2 \tan \beta} \right]^2 = \left(\frac{d}{dx} b(x)_{Wagner} \right)^2 \quad (53)$$

For the present theory the maximum pressure coefficient is taken to be

$$C_{pMax} = \left[\frac{\pi A_b \tan \tau}{2 \tan \beta} \right]^2 = \left(\frac{d}{dx} b(x) \right)^2 \quad (54)$$

Figure 14 compares (53) and (54) together with maxima pressure coefficients from scaling Z&F values and present-theory values from equation (52) at the indicated deadrises. These indicate that very simple formulas depending only on the square of the slope of the waterline, given by $b'(x)$ as taken herein, give excellent values of maxima pressure coefficients. This indicates that the waterline defined by $b(x)$ is correct and that their asymptotic theory yielding (53) applies to the present theory by using the attenuated spray-root offset. Moreover, the values are not much below those of Z&F!

Center of lift—As the distribution of loading is uniform over the length of the waterplane by this theory, the center of lift is at $x = \bar{x} = 2l/3$ aft of apex of the waterplane. This value is in

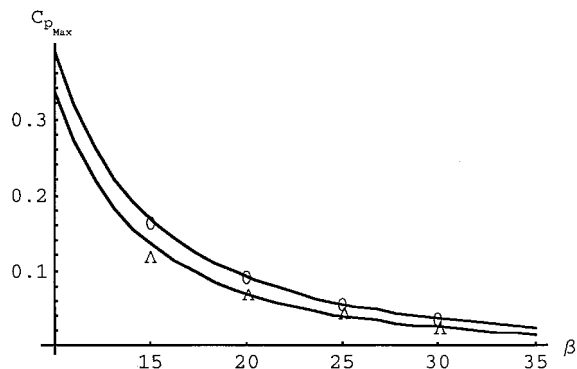


Fig. 14 Maxima pressure coefficients at 4 deg trim as functions of deadrise angle. Circles are from Zhao & Falinsen (1993) applied to planing. Triangles are maxima from current theory, with upper curve equation (53), lower equation (54)

close agreement with Savitsky's empirical fit to data in chines-dry mode at the highest beam Froude number ($U/\sqrt{2gb(l)} = 9$) at which the center of lift is independent of gravity. In current notation, his fit is

$$\bar{x} = \left\{ 1 - \frac{1}{2} \left(\frac{3}{4} - \frac{1}{422A_R^2 + 2.39} \right) \right\} l \quad (55)$$

$= 0.63 \text{ to } 0.65; 1.0 \leq A_R \leq 2.0$

One must expect that the loading falls to zero at the trailing edge and at the apex, where it has long been recognized by aerodynamicists that the slender body fails (see Thwaites (1987)). It is therefore remarkable that the theoretical and experimental results for the lift-centers are as close as they are.

Conclusions

The foregoing demonstrates that development of this theory in an independent, less complicated form confirms, for triangular cross sections, the more general theory as derived by Vorus (1996). Moreover, it is shown for the first time that it agrees *exceptionally well* with all hydrodynamic characteristics determined from well-conducted model experiments within the domain of applicability of slender-body theory. It is also apparent that the old model of Wagner does not predict any of the needed aspects of chines-dry planing with adequate accuracy. It is surprising that the several different models of Zhao & Faltinsen all overestimate pressures and total loadings in spite of their inclusion of much of the nonlinearities. Their corrections to account for three-dimensional effects do not seem to be sufficient to account for the difference with data. Their maximum pressures and those given by the present theory are found to be given by very simple functions of the offsets of the spray roots. The formulas herein show the physically appealing attenuations of the half-breadths with increasing deadrise as defined by the spray-root loci without which the close correlations shown would not be obtained albeit with only one set of data.

Finally, this theory is considered justified to apply in the companion paper, to be published later, to more pragmatic forms without and with camber within the scope of slender-body theory. It is hoped that this development may be extended to higher aspect-ratios and waterplanes with wetted chines to secure semi-empirical fits to existing data on a much more *rational* basis subsequent to the later study, which will be limited to the chines-dry mode.

Acknowledgments

I am indebted to D. Savitsky for his assistance in locating essential references and his sharp views of what is pragmatic in this arena, wherein he has functioned for many years. I am grateful to Eugene Clement (a classmate at Webb Institute of Naval Architecture 1940–44) for proposing the problem to determine the combined effects of camber and deadrise and for provision of many references with J. Koelbel. Discussions with Professor W. Vorus have been most helpful. Professor Faltinsen is thanked for providing several of his more recent papers on impact of sections and planing. This effort could not have been mounted without the generosity of my eldest son, Michael Kevin, who provided a

complete computer system with MATHEMATICA and many other programs. Most certainly long overdue is my expression of gratitude for the education I was privileged to receive at Webb, provided *totally free to all* by the founder, William Henry Webb, a world-class shipbuilder.

References

- BRESLIN, J. P. AND ANDERSEN, P. 1994 *Hydrodynamics of Ship Propellers*. Cambridge University Press, Cambridge, U.K.
- CARLEMAN, T. 1923 Sur les equations integrales singulieres a noyau reel et symmetrique. *Aarsskrift*, **3**, Uppsala, Sweden.
- CLEMENT, E. AND KOELBEL, J. 1992 Optimized designs for stepped planing monohulls and catamarans. Intersociety High Performance Marine Vehicles Conference and Exhibit 92, 1–10.
- CUMBERBACH, E. 1958 Two-dimensional planing at high Froude number. *Journal of Fluid Mechanics*, **4**, 466–478.
- FOUNTAIN, E. AND COINTE, R. 1997 Etude de l'écoulement autour d'un navire planant. 6e Ecole Centrale, Nantes, France, 3–16.
- GRADSTEYN, I. S. AND RYZHIK, I. M. 1980 *Table of integrals, series and products*. Academic Press, London.
- LIXIN, X., TROESCH, A. W., AND VORUS, W. S. 1998 Asymmetrical vessel impact and planing hydrodynamics. *JOURNAL OF SHIP RESEARCH* **42**, 3, 187–198.
- MARUO, H. 1951 *Proceedings*, First Japan National Congress of Applied Mechanics, 409–422.
- MARUO, H. 1959 *Journal of Zosen Kiokai*.
- MARUO, H. 1967 High-and-low-aspect ratio approximation of planing surfaces. *Schiffstechnik*, **14**, 72, 57–64.
- MOORE, W. 1967 Cambered planing surfaces for stepped hulls; some theoretical and experimental results. DTMB Rpt. 2387, Feb.
- NEWMAN, J. N. 1977 *Marine Hydrodynamics*. The MIT Press, Cambridge, Mass.
- PIERSON, J. D., DINGEE, D. A., AND NEIDINGER, J. W. 1954 A hydrodynamic study of the chines-dry planing body. Experimental Towing Tank, Davidson Laboratory Report 492, Hoboken, New Jersey.
- SAVITSKY, D. 1964 Hydrodynamic design of planing hulls. *Marine Technology*, **1**, 1, 71–95.
- SAVITSKY, D. AND GORE, J. L. 1979 A re-evaluation of the planing hull form. AIAA/SNAME Advanced Marine Vehicles Conference, Baltimore, Md., 145–159.
- SOTTORF, W. 1934 Experiments with planing surfaces. Tech. Memorandum No. 735 National Advisory Committee for Aeronautics (now NASA), Washington, DC.
- THWAITES, B. 1987 *Incompressible Aerodynamics*. Dover Publications, New York.
- TRICOMI, F. G. 1985 *Integral Equations*. Dover Publications, New York.
- TULIN, M. 1957 The theory of slender planing surfaces at high speed. *Schiffstechnik*, **4**, 21, 125–133.
- VAN MANEN, J. D. AND VAN OOSSANEN, P. 1988 in "Resistance," *Principles of Naval Architecture*, SNAME, E. Lewis, Ed., **2**, Chapter V, Section 3, 11.
- VORUS, W. S. 1996 A flat cylinder theory for vessel impact and steady planing resistance. *JOURNAL OF SHIP RESEARCH*, **40**, 2, June, 89–106.
- WAGNER, H. 1932 Über Stoss- und Gleitvorgänge an der Oberfläche von Flüssigkeiten, *Zeitschrift für Angewandte Mathematik und Mechanik*, Ingenieurwissenschaftliche Forschungsarbeiten, Berlin, **12**, 4, 194–215.
- WU, T. Y. AND WHITNEY, A. K. 1972 Theory of optimum shapes in free-surface flows. Part 1. Optimum profile of sprayless planing surface. *Journal of Fluid Mechanics*, **55**, 3, 439–454.
- ZHAO, R. AND FALTINSEN, O. 1993 Water entry of two dimensional bodies. *Journal of Fluid Mechanics*, **246**, 593–612.
- ZHAO, R., FALTINSEN, O., AND AARSNES, J. 1996 Water entry of arbitrary two-dimensional sections with and without flow separation. *Proceedings*, 21st Symposium on Naval Hydrodynamics, Trondheim, Norway, U.S. National Academy of Science Press, Washington, DC.
- ZHAO, R., FALTINSEN, O., AND HASLUM, H. A. 1998 A simplified nonlinear analysis of a high-speed planing craft in calm water. *Proceedings*, FAST '97, 431–438.